J. Cent. South Univ. (2013) 20: 2643−2649
DOI: 10.1007/s11771-013-1779-1

Springer

Microstructure and mechanical properties of high speed indirect-extruded Mg-5Sn-(1,2,4)Zn alloys

CHENG Wei-li(程伟丽)[1, 2], WANG Miao(王淼)[2], QUE Zhong-ping(阙仲萍)[1, 2], XU Chun-xiang(许春香)[2], ZHANG Jin-shan(张金山)[2], LIANG Wei(梁伟)[1, 2], YOU Bong-sun[3], PARK Sung-soo[4]

1. Key Laboratory of Interface Science and Engineering in Advanced Materials of Ministry of Education (Taiyuan University of Technology), Taiyuan 030024, China;
2. School of Materials Science and Engineering, Taiyuan University of Technology, Taiyuan 030024, China;
3. Korea Institute of Materials Science, Changwon 641-831, Korea;
4. Ulsan National Institute of Science and Technology, Ulsan 689-798, Korea

Abstract: The microstructural evolution and mechanical properties of high speed indirect-extruded Mg-5%Sn-(1, 2, 4) Zn (mass fraction, %) alloys were investigated by optical microscopy (OM), X-ray diffraction (XRD), scanning electron microscopy (SEM), differential thermal analysis (DTA) and a static tension tester. All the studied alloys can be extruded successfully at a high speed of 10 m/min. The grain size, area fraction of particles and tensile properties are found to be greatly affected by the extrusion speed and Zn content, resulting in tensile properties showing lower strength and ductility as the extrusion speed increases and Zn content decreases. The dependence of grain size and tensile properties on the second phase particles is also discussed.

Key words: magnesium alloy; indirect extrusion; microstructure; mechanical properties

1 Introduction

Recently, significant interest exists in the development of novel wrought magnesium alloys due to the strong demands for weight reduction in the automotive and aerospace industries. However, the application of wrought magnesium alloys, especially extruded magnesium alloys, in industrial applications, is still limited due to their low strength and poor formability at low temperature [1−3]. Generally, high-strength Mg alloys such as AZ80 and AZ91 are extrudable only at speeds of 0.5−2.5 m/min in the temperature range of 300−450 ºC, well below those attainable with Al alloys [3]. This is mainly due to an increase in the susceptibility to hot shortness during extrusion with increases in alloying element such as Al caused by the incipient melting of second-phase particle. In this respect, it is believed that Mg-Sn based alloys have huge potential for use in high-speed extrusion processes, as they usually have higher incipient melting temperature than conventional AZ alloy system [4−6]. Furthermore, the indirect extrusion has many advantages over direct extrusion and it is expected to be a feasible implementation at lower temperature and higher extrusion speed [3, 7]. Recently, it has been reported that Mg-Sn based alloys are readily extrudable at low temperature and they exhibit excellent mechanical properties after extrusion [8–10]. However, the extrusion speeds tried so far have only been in a range of 0.12−2 m/min, which means that the potential of these alloys for high-speed extrusion processes have not been fully explored. In addition, SASAKI et al [4] and TANG et al [10] indicated that the addition of Zn to Mg-Sn based alloys could enhance the mechanical performance by microstructure refinement and second phase morphology modification. In the present work, therefore, experimental Mg-5Sn-(1,2,4)Zn (mass fraction, %) alloys were subjected to extrusion at a high extrusion speed (HES) of 10 m/min and the microstructure and mechanical properties of extruded alloys were investigated and compared to those of ones extruded at a low extrusion speed (LES) of 2 m/min.

Foundation item: Project(2012R1A1A1012802) supported by Basic Science Research Program through the National Research Foundation (NRF) of Korea funded by the Ministry of Education, Science and Technology; Project(2013021013-4) supported by Shanxi Province Science Foundation for Youths, China; Project supported by Advanced Programs of Department of Human Resources and Social Security of Shanxi Province for Returned Scholars; Project(2012L003) supported by Foundation for Young Scholars of Taiyuan University of Technology, China
Received date: 2012−07−01; **Accepted date:** 2012−11−15
Corresponding author: PARK Sung-soo, Assistant Professor, PhD; Tel: +82−52−217−2328; E-mail: sspark@unist.ac.kr

2 Experimental

Alloy of nominal composition of Mg-5Sn (mass fraction, %), with systematic additions of 1%, 2% and 4% Zn (mass fraction), was prepared from high purity (99.9%) Mg, Sn, and Zn by induction melting in a cemented graphite crucible at approximately 700 ºC under a CO_2+SF_6 atmosphere and casting into a steel mould pre-heated to 200 ºC. The analyzed and nominal compositions of Mg-5Sn-(1,2,4) Zn alloys used in this work are listed in Table 1. Billet was given a homogenization treatment at 420 ºC for 24 h, followed by immediate cold water cooling. The dimension of the billet was 80 mm in diameter and 200 mm in length. Indirect extrusion experiments were implemented at an initial billet temperature of 250 ºC and at exit speeds of 2 and 10 m/min, respectively. A rod profile was extruded with a fixed extrusion ratio (ER) of 50, in other words, under a constant strain. Microstructure examinations were conducted in midsection parallel to the extrusion direction (ED). All samples for optical microscopy (OM) were sectioned, cold-mounted, polished and then etched in a solution of picric and acetic acid for 15−30 s. The average grain size and area fraction of second phase were analyzed from several micrographs using a computer-aided liner intercept measurement. The scanning electron microscopy (SEM) was carried out on a JEOL 5800 at 20 kV. Phase analysis was conducted by X-ray diffraction (XRD). Thermal analysis was performed using a HCT-2 differential thermal analyzer at a heating rate of 5 °C/min. For tensile testing, specimen with 25 mm in gage length and 5 mm in gage diameter was machined from the rod. All the quasi-static tensile tests were performed at a strain rate of 10^{-3} s^{-1} on INSTRON-4206 static tension tester.

Table 1 Nominal (analyzed) chemical composition of studied alloys (mass fraction, %)

Alloy	Nominal (analyzed) composition		
	Sn	Zn	Mg
TZ51	5 (4.95)	1 (1.02)	Bal.
TZ52	5 (4.98)	2 (1.95)	Bal.
TZ54	5 (4.97)	4 (3.96)	Bal.

3 Results and discussion

3.1 Microstructure characteristics of homogenized TZ51/2/4 alloys

Figure 1 shows the optical micrographs of homogenized TZ51/2/4 alloys. They all consist of α-Mg grains with sizes ranging from 167 (TZ51) to 102 μm (TZ54) and some black particles that remain undissolved after homogenization. The area fraction of black particles increases from 0.3% to 1.2% as Zn content increases from 1% to 4%. The diminishing grain size with Zn content is associated with the increasing area fraction of black particles on the grain boundary, which can act as barriers to grain growth.

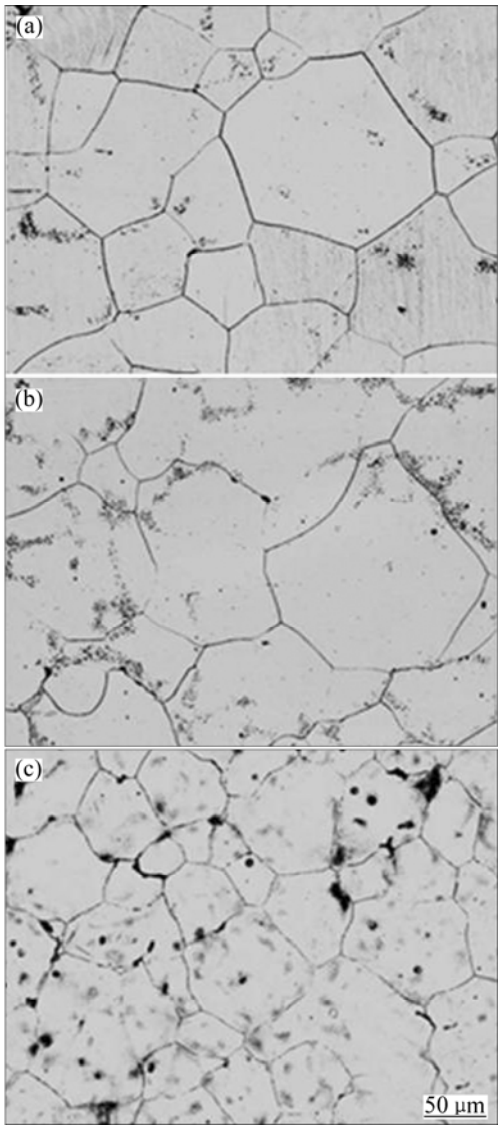

Fig. 1 Optical micrographs of as-homogenized alloys: (a) TZ51; (b) TZ52; (c) TZ54

Figure 2 shows the XRD and SEM-EDS results of the homogenized alloys. As indicated, the particles in the TZ51 and TZ52 alloys are mostly Mg_2Sn in despite that few MgZn phase also exists in the matrix, while those in TZ54 mainly consist of both Mg_2Sn and MgZn phases. It should be noted that some Zn segregation areas can be observed around the massive Mg_2Sn phase in TZ54 alloy, indicating that Zn can provide the heterogeneous nucleation sites for the formation of Mg_2Sn phase.

3.2 Microstructure characteristics of extruded TZ51/2/4 alloys

Figure 3 shows the optical micrographs of the studied alloys extruded at two different extrusion speeds (i.e., 2 and 10 m/min). The extruded alloys show considerably refined equiaxed grains, which is mainly a

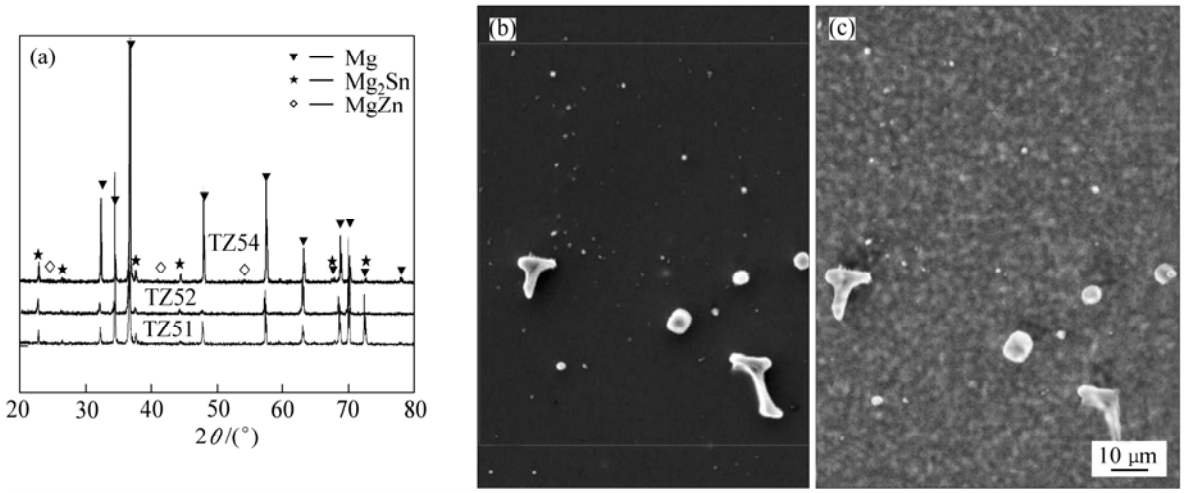

Fig. 2 XRD patterns of TZ51/2/4 alloys (a), SEM micrograph (b) and elements dot-mapping (c) of as-homogenized TZ54 alloy

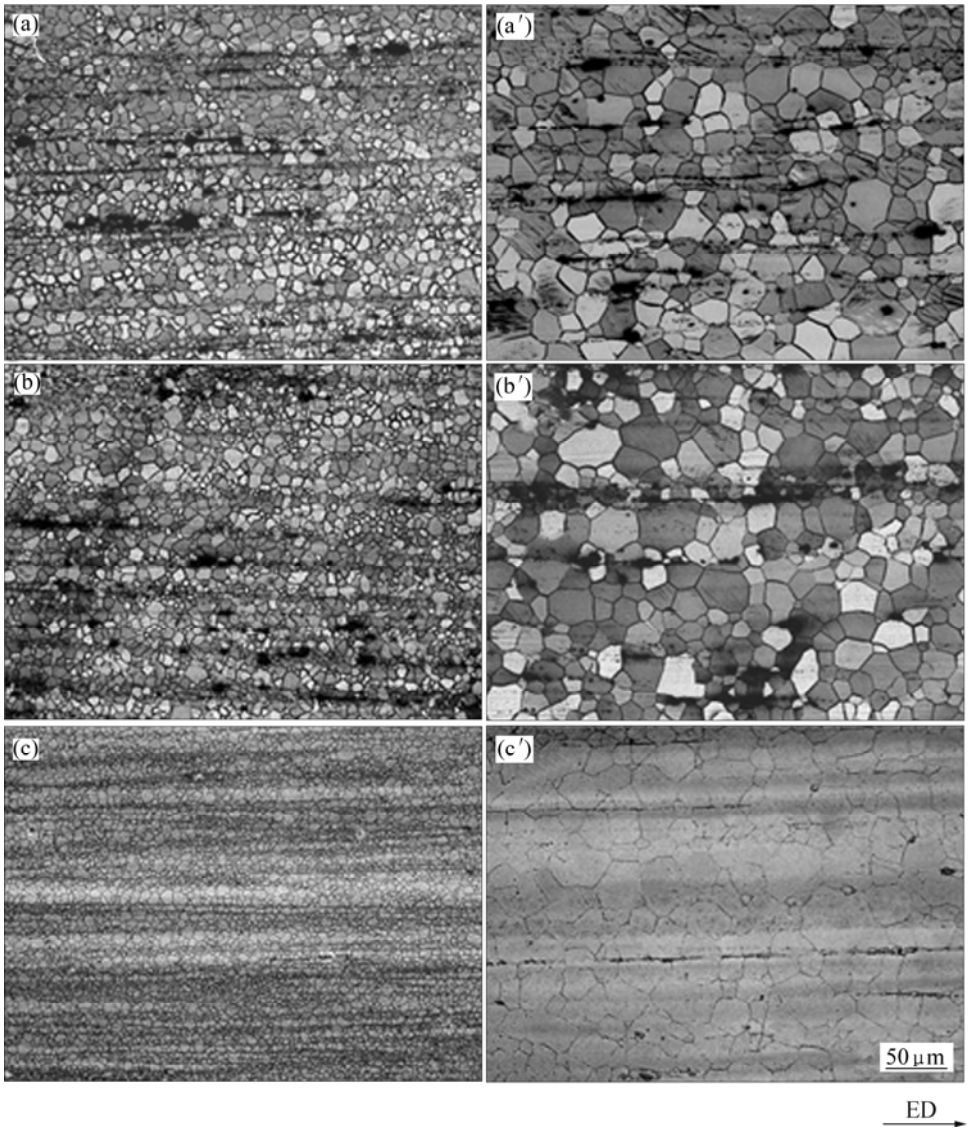

Fig. 3 Optical micrographs of as-extruded alloys: (a), (b), (c) 2 m/min; (a′), (b′), (c′) 10 m/min; (a), (a′) TZ51; (b), (b′) TZ52; (c), (c′) TZ54

consequence of dynamic recrystallization during the extrusion process. Furthermore, the Mg_2Sn particles are found to be aligned along the ED in the form of stringers after being broken into fragments during the extrusion process [9, 11]. The difference in grain size caused by extrusion speed for equivalent starting material in the present work is broadly apparent. Generally, the grain sizes of the alloys extruded at HES of 10 m/min are almost two times bigger than those of the alloys extruded at LES of 2 m/min. Nevertheless, the effect of Zn content on the grain size is not obvious in fixed extrusion condition. For the case studied here, the grain sizes decrease slightly with increasing Zn content. The average grain sizes of the studied alloys extruded at two different speeds are listed in Table 2.

Figure 4 shows the SEM micrographs of the

Table 2 Mechanical properties of as-extruded alloys

Alloy	YS/MPa	UTS/MPa	Elongation/%	Work-hardening capacity (UTS/TYS)	Grain size/μm	Area fraction of fine particles/%
TZ51 (2 m/min)	154	242	18.5	1.57	8.1	1.74
TZ52 (2 m/min)	156	258	23.3	1.65	7.6	2.03
TZ54 (2 m/min)	156	284	25.3	1.82	7.3	8.27
TZ51 (10 m/min)	130	230	15	1.77	16.1	1.12
TZ52 (10 m/min)	132	235	15.3	1.78	15.8	1.75
TZ54 (10 m/min)	131	258	23.1	1.97	15.6	2.04

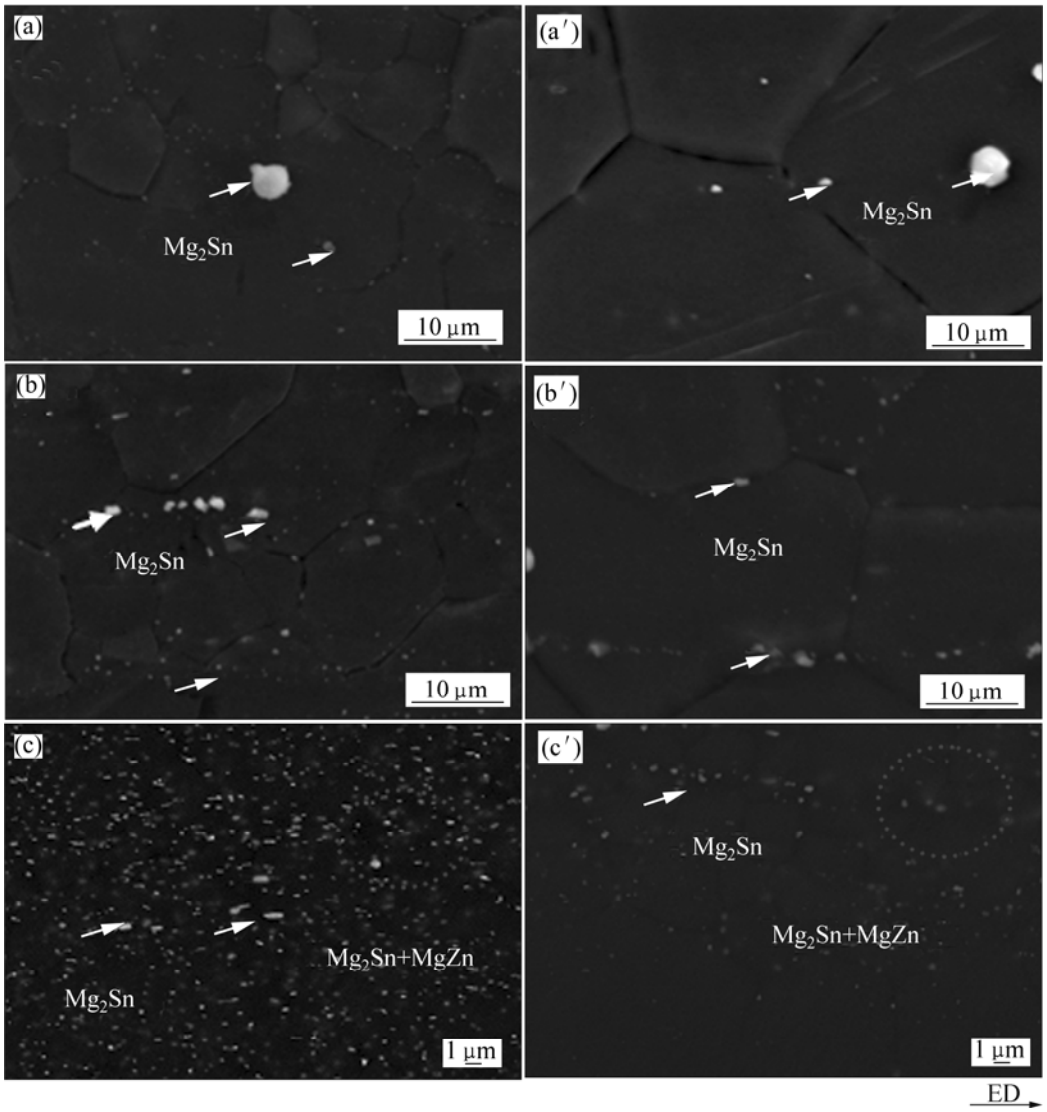

Fig. 4 SEM micrographs of as-extruded alloys; (a), (b), (c) 2 m/min; (d), (e), (f) 10 m/min; (a), (a′) TZ51; (b), (b′) TZ52; (c), (c′) TZ54

extruded alloys. As indicated, some coarse particles with sizes of more than 1 μm can be identified as the same phase observed in the homogenized condition. Note that relatively fine particles with sizes of less than 1 μm, which are not present prior to extrusion, are distributed in α-Mg matrix. Similar results on the formation of fine particles during extrusion have been reported in precipitation-hardenable Mg alloys, and are attributed to dynamic precipitation [8−9]. During the extrusion process, dislocations caused by plastic deformation can accelerate the precipitation kinetics by providing nucleation sites and increasing the diffusion rate of alloying elements in the alloys. The main microstructural difference is observed in the area fraction of second-phase particles. In general, the area fractions of these particles tend to increase as the extrusion speed decreases and/or the Zn content increases. As the case with the homogenized alloys, the presence of fine particles is seen to be beneficial to maintaining fine grain size. This would be possible via suppression of grain growth by the Zener drag [12]. This so-called Zener effect increases with increasing the number of particles and decreasing the particle size. Therefore, TZ54 alloy extruded in LES condition with the largest area fraction of fine particles exhibits the finest grain size among the studied alloys. Moreover, the grains become coarser in HES alloys with lower area fraction of fine particles compared to those of corresponding LES alloys, as shown in Table 2.

Figure 5(a) shows the XRD patterns of TZ54 alloys extruded at two different extrusion speeds. As exhibited, the extruded TZ54 alloy is mainly composed of α-Mg, MgZn and Mg_2Sn phases. It should be noted that the peaks corresponding to Mg_2Sn of the HES alloy are weaker than those of LES one, implying that the area fraction of Mg_2Sn decreases as extrusion speed increases. Furthermore, the incipient temperature of MgZn phase is lower compared to that of Mg_2Sn [7]. This can also be verified in the DTA curves (Fig. 5(b)) of TZ51 and TZ54 alloys extruded in the same condition. As exhibited, the incipient temperature of second phase and melting temperature of the alloys decrease as Zn content increases, namely the occurrence of MgZn phase reduces the thermal stability of the alloy. Under the HES condition, on one hand, the high extrusion speed increases the die exit temperature and leads to grain growth and the dissolution of MgZn phase into the matrix. On the other hand, the high extrusion speed reduces the area fractions of dynamically precipitated Mg_2Sn particles due to the limited time for Sn diffusion and the diminishing nucleation sites provided by Zn during extrusion processing. Therefore, the Zener effect

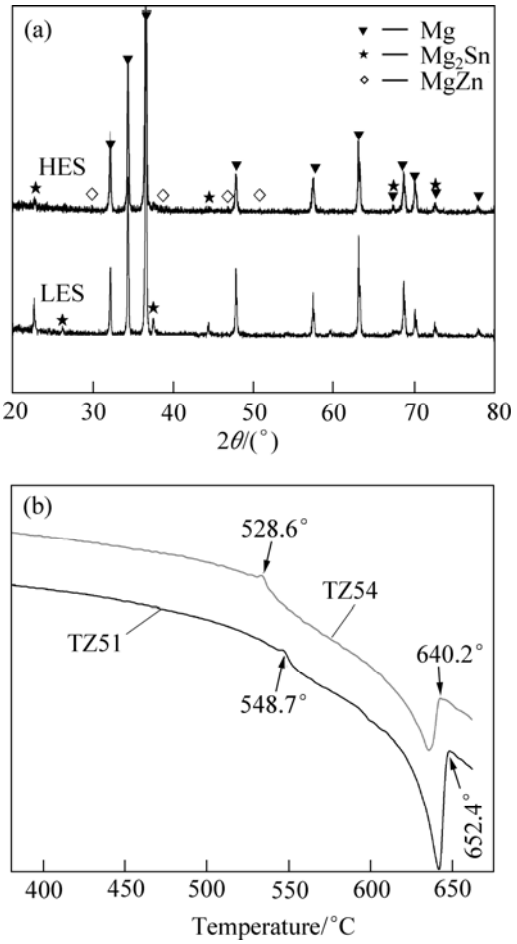

Fig. 5 XRD patterns and DTA curves of as-extruded alloys: (a) TZ54 (2 and 10 m/min); (b) TZ51 and TZ54 (2 m/min)

is weakened and grain growth is more active during the high extrusion speed processing. This is ascribed to the grain coarsening of the HES alloys compared to the LES ones.

3.3 Tensile properties of extruded TZ51/2/4 alloys

Figures 6(a) and (b) show the engineering stress−strain curves of the extruded rods in tension. The tensile properties of the tested alloys are also summarized in Table 2. All the stress−strain curves have a special characteristic in common: they all reveal a flow stress maximum followed by a conspicuous loss of strength. As exhibited, tensile yield strength (TYS) and ultimate tensile strength (UTS) increase with increasing Zn content regardless of HES and LES specimens. Note that the increments in TYS are not so obvious as those in UTS. The increasing UTS indicates that the degree of work-hardening increases with increasing the Zn content. The work-hardening capacity, defined as the ratio of UTS to TYS, is measured to evaluate the work-hardening degree [10, 13]. For both LES and HES specimens, the values appear to increase as the Zn content increases

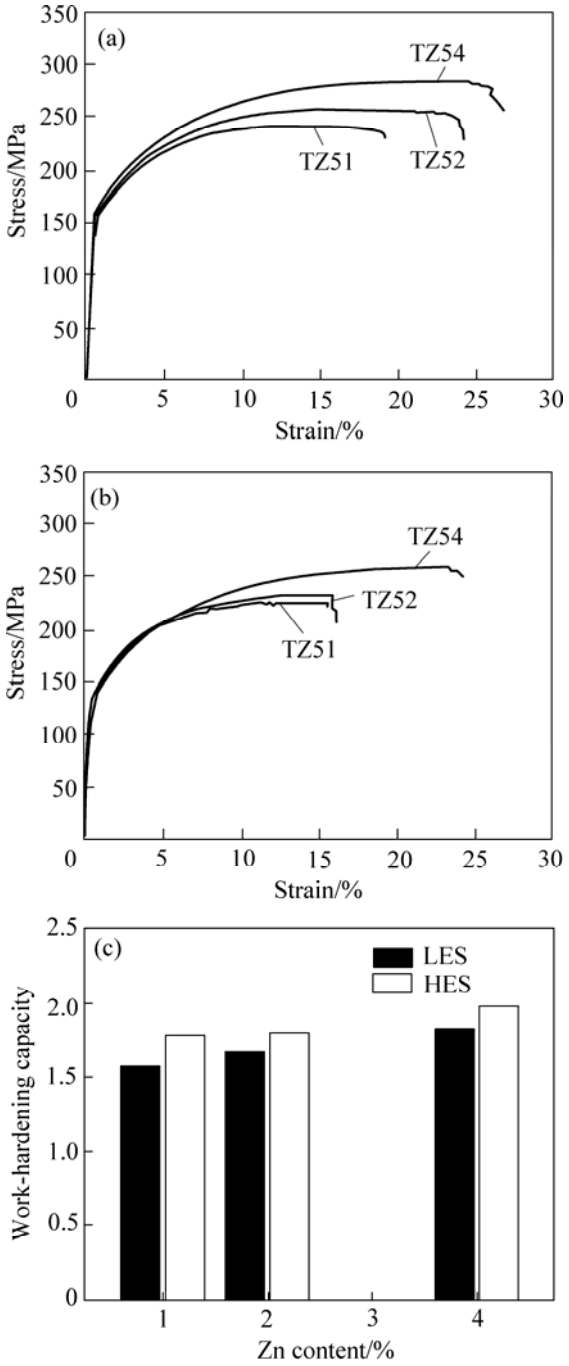

Fig. 6 Engineer strain−stress curves and work-hardening capacity of as-extruded alloys: (a) Engineer strain−stress curves of studied alloys extruded at 2 m/min (LES); (b) Engineer strain−stress curves of studied alloys extruded at 10 m/min (HES); (c) Work-hardening capacity of LES and HES alloys

from 1.57% to 1.82% in LES condition and from 1.77% to 1.97% in HES condition. The variation of work-hardening capacity with Zn content and extrusion speed may be related to the grain size and precipitates, respectively. The variation of work-hardening capacity with Zn content and extrusion speed is shown in Fig. 6(c), where grain size and area fraction of precipitates are also included.

As also observed in Fig. 6 and Table 2, as the extrusion speed increases, both strength and ductility deteriorate, which is different from the typical relationship between strength and ductility [1]. The decrease in strength with increasing extrusion speed is mainly due to the reduced grain boundary strengthening, following the Hall-Petch relationship. Very recently, our previous work [14] indicated that the decrease in ductility of high speed extruded Mg-Sn based alloys was associated with the occurrence of double twining during tensile test. It has been well known that double twinning accelerates cracking, which is induced by dislocation pile-ups at the twin/matrix interface [15]. Among the studied alloys, TZ54 alloy exhibits the best combined properties. The relatively high strength and good ductility of TZ54 alloy is mainly due to the second phase strengthening and fine-grain strengthening resulted from the more and finer dispersed particles and smaller grain size, respectively.

4 Conclusions

1) Mg-5Sn-(1,2,4)Zn (mass fraction, %) alloys are demonstrated to be extrudable at a relatively high extrusion speed of 10 m/min and with a high ratio of 50.

2) The grain size, area fraction and morphology of second phase particles are found to be significantly influenced by the extrusion speed and Zn content, resulting in tensile properties showing lower strength and ductility as the extrusion speed increases and Zn content decreases.

3) The relatively high strength and good ductility of TZ54 alloy is mainly due to the second phase strengthening and fine-grain strengthening resulted from the more and finer dispersed particles and smaller grain size, respectively.

References

[1] BETTLES C J, GIBSON M A. Current wrought magnesium alloys: Strengths and weaknesses [J]. JOM, 2005, 57(5): 46−49.

[2] KANG D H, PARK S S, KIM N J. Development of creep resistant die cast Mg-Sn-Zn-Al alloy [J]. Mater Sci Eng A, 2005, 413/4(1): 555−560.

[3] PARK S S, YOU B S, YOON D J. Effect of the extrusion conditions on the texture and mechanical properties of indirect-extruded Mg-3Al-1Zn alloy [J]. Journal of Materials Processing Technology, 2009, 209: 5940−5943.

[4] SASAKI T T, YAMAMOTO K, HONMA T, KAMADO S, HONO K. A high-strength Mg-Sn-Zn-Al alloy extruded at low temperature [J]. Scripta Materialia, 2008, 59: 1111−1114.

[5] MENDIS C L, BETTLES C J, GIBSON M A, HUTCHINSON C R. An enhanced age hardening response in Mg-Sn based alloys containing Zn [J]. Mater Sci Eng A, 2006, 435/436(1): 163−171.

[6] LIU Hong-mei, CHEN Yun-gui, TANG Yong-bai, WEI Shang-hai, NIU Gao. The microstructure, tensile properties, and creep behavior of as-cast Mg-(1–10)%Sn alloys [J]. Journal of Alloys and Compound, 2007, 440(1/2): 122−126.

[7] WU Y, PARK Y W, PARK H S, HWANG S K. Microstructural development of indirect-extruded TiAl-Mn-Mo-C intermetallic alloys during aging [J]. Materials Science Engineer A, 2003, 347(1/2): 171−179.

[8] PARK S S, TANG W N, YOU B S. Microstructure and mechanical properties of an indirect-extruded Mg-8Sn-1Al-1Zn alloy [J]. Materials Letters 2010, 64(1): 31−34.

[9] CHENG W L, PARK S S, YOU B S, KOO B H. Microstructure and mechanical properties of binary Mg-Sn alloys subjected to indirect extrusion [J]. Materials Science Engineer A, 2010, 527(18/19): 4650−4653.

[10] TANG W N, PARK S S, YOU B S. Effect of the Zn content on the microstructure and mechanical properties of indirect-extruded Mg-5Sn-*x*Zn alloys [J]. Materials and Design, 2011, 32(6): 3537−3543.

[11] BALL E A, PRANGNELL P B. Tensile-compressive yield asymmetries in high strength wrought magnesium alloys [J]. Scripta Metallurgica et Materialia, 1994, 31(2): 111−116.

[12] HOMMA T, KUNITO N, KAMADO S. Fabrication of extraordinary high-strength magnesium alloy by hot extrusion [J]. Scripta Materialia, 2009, 61(6): 644−647.

[13] KIM S K, KIM Y M, LIM Y J, KIM N J. Relationship between yield ratio and the mechanical constants of the swift equation [J]. Metals and Materials International, 2006, 12(2): 131−135.

[14] CHENG W L, KIM H S, YOU B S, KOO B H, PARK S S. Strength and ductility of novel Mg-8Sn-1Al-1Zn alloys extruded at different speeds [J]. Materials Letters, 2011, 65(11): 1525−1527.

[15] BARNETT M R. Twinning and the ductility of magnesium alloys. Part II: “Contraction” twins [J]. Materials Science Engineer A, 2007, 464(1/2): 8−16.

(Edited by YANG Bing)